

Kink propagation in the Artificial Axon

Xinyi Qi and Giovanni Zocchi*

Department of Physics and Astronomy, University of California - Los Angeles

The Artificial Axon is a unique synthetic system, based on biomolecular components, which supports action potentials. Here we consider, theoretically, the corresponding space extended system, and discuss the occurrence of solitary waves, or kinks. In contrast to action potentials, stationary kinks are possible. We point out an analogy with the interface separating two condensed matter phases, though our kinks are always non-equilibrium, dissipative structures, even when stationary.

Introduction. The Artificial Axon (AA) is a synthetic structure designed to support action potentials, thus generating these excitations for the first time outside the living cell. The system is based on the same microscopic mechanism as that operating in neurons, the basic components being: a phospholipid bilayer with embedded voltage gated ion channels, and an ionic gradient as the energy source. However, while a real axon has at least two ion channel species and opposite ionic gradients across the cell membrane, the AA has only one. In the experiments, a current limited voltage clamp (CLVC) takes the role of a second ionic gradient [1, 2]. The experimental system in [2] is built around a $\sim 100 \mu\text{m}$ size black lipid membrane. As a dynamical system for the voltage, it operates in zero space dimensions (similar to the "space clamp" setup with real axons [3, 4]). That is, each side of the membrane is basically an equi-potential surface (the name Artificial Axon, while a misnomer in this respect, is historical [1] and we propose to keep it for the original and future versions). Inspired by this system, here we consider - theoretically - the corresponding space extended dynamical system. We focus on the existence of solitary wave solutions, or propagating kinks (we will use the two terms interchangeably, to mean a front which propagates keeping its shape). Kinks appear in many areas of condensed matter physics [5], from domain walls in magnetic materials [6, 7] to pattern forming chemical reactions [8]. Our particular nonlinear structures come from a dissection, so to speak, of the mechanism of action potential generation. We show the existence of travelling kinks in our system, and study numerically their characteristics in relation to the control parameters, which are the command voltage and the conductance of the CLVC. Then we discuss a "normal form" for this class of dynamical systems, highlighting the relation with other kinks separating two condensed matter phases, such as the nematic - isotropic interface in liquid crystals. The nonlinearities which thus arise retrace the development of simplified models of the Hodgkin-Huxley axon [9], such as introduced 60 years ago by Fitzhugh [10] and Nagumo et al [11]. Looking at kinks thus provides a somewhat different perspective on a classic topic in the study of excitable media.

Results. We consider the AA in one space dimension. The physical system we have in mind is a $\sim 1 \text{ cm}$ long, $\sim 100 \mu\text{m}$ wide supported strip of lipid bilayer with one species of voltage gated ion channels embedded. The bilayer might be anchored to the solid surface so as to leave a sub-micron gap (the "inside" of the axon) in between. At present, the stability of the bilayer stands in the way of a practical realization, but this problem is not unsurmountable. The bilayer acting essentially like the dielectric in a parallel plates capacitance, the local charge density is related to the voltage by $(\partial/\partial t)\rho(x, t) = c(\partial/\partial t)V(x, t)$ where c and ρ are capacitance and charge per unit length, respectively. The current inside the axon follows Ohm's law: $j = -(1/r)(\partial V/\partial x)$ where r is the resistance per unit length; then charge conservation leads to the diffusion equation for the potential: $(\partial V(x, t)/\partial t) - (1/(rc))(\partial^2 V(x, t)/\partial x^2) = 0$. In the AA, an ionic gradient (of K^+ ions) across the membrane leads to an equilibrium (Nernst) potential $V_N = (T/|e|) \ln([K^+]_{out}/[K^+]_{in})$, but the system is held off equilibrium by the current injected through a current limited voltage clamp (CLVC) [1]. The active elements are voltage gated potassium channels inserted in the membrane: these are molecular pores which, in the open state, selectively conduct K^+ ions. The KvAP channel used in [2, 12] has three functionally distinct states: open, closed, and inactive; the presence of the inactive state allows the system to generate action potentials. Here we consider the simpler case of a "fast" channel with no inactivation. Then the channels can be described by an equilibrium function $P_O(V)$ which gives the probability that the channel is open if the local voltage is V . Introducing the current sources in the diffusion equation above one arrives at the following $(1+1)D$ dynamical system:

$$\frac{\partial V(x, t)}{\partial t} - \frac{1}{rc} \frac{\partial^2 V}{\partial x^2} = \frac{\chi}{c} P_O(V) [V_N - V(x, t)] + \frac{\chi_c}{c} [V_c - V(x, t)] \quad (1)$$

V is the voltage inside the axon (referred to the grounded outside), and we assume a distributed "space clamp" for the CLVC (this would be provided by an electrode along the axon). Eq. (1) is of the general form of a reaction - diffusion system; these are usually studied in the context of pattern forming chemical reactions. For us it represents a continuum limit, i.e. we consider a

* zocchi@physics.ucla.edu

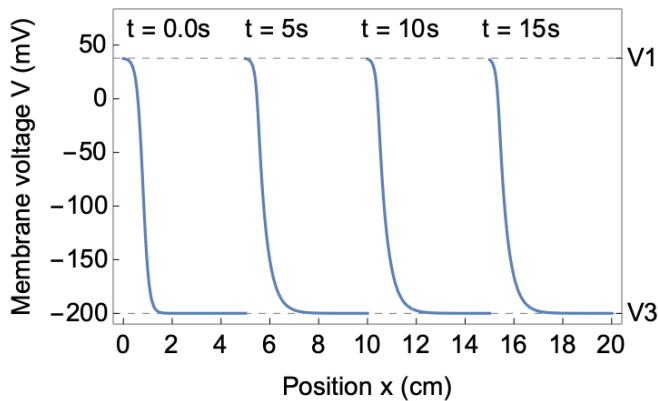


FIG. 1. The traveling kink solution $V(x, t)$ for (1), (2). The plot shows snapshots of the kink at different times; the initial condition ($t = 0$) is a hyperbolic tangent. Parameter values are those given in the text, with a clamp voltage $V_c = -200 mV$. The dotted horizontal lines show the fixed points V_1 and V_3 . Notice that the shape of the kink shifts from the initial condition at $t = 0.0s$ to a stable shape afterwards.

uniform, distributed channel conductance instead of discrete, point-like ion channels. This is a mean field approximation which neglects correlations between nearby channels. The first term on the RHS of (1), when multiplied by c , is the channel current, proportional to the driving force ($V_N - V$); V_N is the Nernst potential, χ the conductance (per unit length) with channels open (i.e. $\chi = n\chi_0$, χ_0 single channel conductance, n number of channels per unit length). The second term is the current injected by the clamp; V_c is the clamp voltage (which is a control parameter in the experiments), χ_c the clamp conductance (per unit length), which is a second control parameter. The function $P_O(V)$ is a Fermi-Dirac distribution:

$$P_O(V) = \frac{1}{\exp[-q(V - V_0)/T] + 1} \quad (2)$$

where q is an effective (positive) gating charge and V_0 the midpoint voltage where $P_O(V_0) = 1/2$. To fix ideas, we will use parameters consistent with the AA in [12]: $V_N = 50 mV$, $\chi/c = 100 s^{-1}$, $\chi_c/c = 5 s^{-1}$, $(1/rc) = 1 cm^2/s$, $V_0 = -10 mV$, $q/T = 0.08 (mV)^{-1}$. We use Gaussian units except that we express voltages in mV : this is more convenient to relate to experimental systems. Also, the temperature in (2) and elsewhere is in energy units; thus at room temperature $T/|e| \approx 0.025 mV$ where e is the charge of the electron.

The possibility of travelling kink solutions of (1) and (2) arises because, with the clamp at a negative voltage, say $V_c = -100 mV$, there is a fixed point of (1) (a uniform, time independent solution) with $V(x, t) \approx V_N$ and open channels ($P_O(V) \approx 1$), namely $V = V_1 \approx (\chi V_N + \chi_c V_c)/(\chi + \chi_c)$. A second fixed point is $V(x, t) = V_3 \approx V_c$ and channels closed ($P_O(V) \approx 0$). A stable kink solution

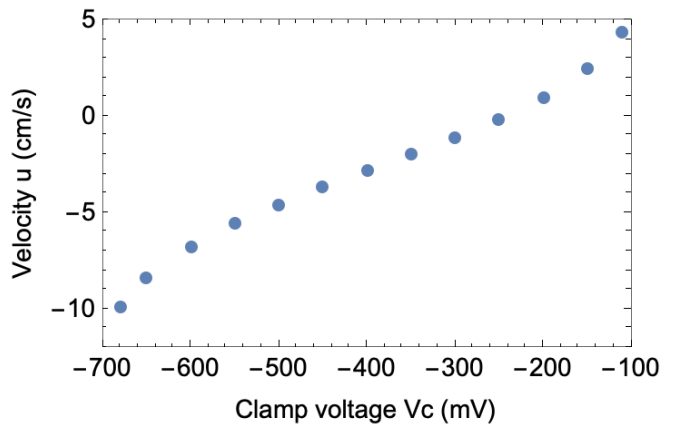


FIG. 2. Plot of kink velocity vs clamp voltage. Parameter values are those given in the text. The velocity is determined by tracking the minimum of the first derivative of $V(x, t)$, which corresponds to the inflection point of the kink-shaped wave front. The left most and right most data points are close to the values of V_c beyond which the kink solution disappears. The graph is asymmetric with respect to right moving and left moving kinks.

exists, asymptotically connecting these two stable fixed points (a third fixed point is unstable and will be discussed later). The essential parameters in (1) are the diffusion constant $D \equiv 1/(rc)$ and χ/c ; from these we can form a characteristic length scale $\Delta = 1/\sqrt{r\chi}$ which gives the scale of the width of the kink solution, and a characteristic velocity $v = D/\Delta = (1/c)\sqrt{\chi/r}$ which similarly gives the scale for the kink velocity. With the parameters above, $\Delta \approx 1 mm$ and $v \approx 10 cm/s$. Fig. 1 shows snapshots of a travelling kink obtained by integrating (1), (2) using the parameters above and $V_c = -200 mV$. The kink was launched with a hyperbolic tangent initial condition ($t = 0$ trace in Fig. 1); it is found to quickly (on a time scale $\sim c/\chi$) attain a stable limiting shape and thereafter travel at constant velocity. The velocity depends on the clamp voltage V_c , as shown in Fig. 2. We measure it by tracking the inflection point of the solution $V(x, t)$. The solitary wave solution exists only for V_c within certain bounds; correspondingly there is a maximum velocity of the kink, while the minimum velocity is zero, as we show below.

Let us now analyze these solitary wave solutions (see e.g. [5]). Eq. (1) is of the form:

$$\frac{\partial V(x, t)}{\partial t} - \frac{\partial^2 V}{\partial x^2} = g(V) \quad (3)$$

where we have changed to non-dimensional variables using $\Delta = 1/\sqrt{r\chi}$, $\tau = c/\chi$, V_N as the units of length, time, and potential, respectively. Then,

$$\begin{cases} g(V) = P_O(V)[1 - V] + \frac{\chi_c}{\chi} \left[\frac{V_c}{V_N} - V \right] \\ P_O(V) = \left\{ \exp\left[-\frac{qV_N}{T}(V - \frac{V_0}{V_N})\right] + 1 \right\}^{-1} \end{cases} \quad (4)$$

We look for a travelling wave solution: $V(x, t) = \varphi(x - ut) = \varphi(z)$, $z \equiv x - ut$; then from (3):

$$\varphi'' + u\varphi' = -\frac{d}{d\varphi}F(\varphi) \quad (5)$$

where F is the primitive of g , i.e. $g(\varphi) = dF/d\varphi$. We may interpret (5) as the equation of motion of a unit mass in a potential energy F , subject to a frictional force proportional to the velocity. The dissipation parameter u is the velocity of the kink. In Fig. 3 we plot the function F obtained from integrating g in (4); the analytic expression, which involves the poly log function, is readily obtained with Mathematica.

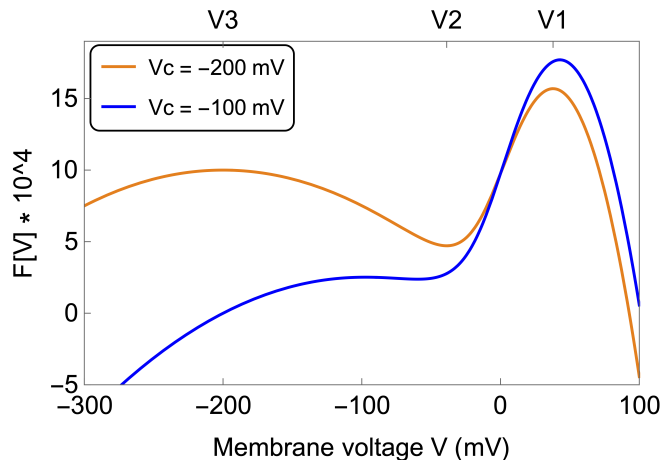


FIG. 3. The function $F(\varphi)$ obtained from (4) vs the (dimensional) membrane voltage, for clamp voltages of -100 mV and -200 mV. Parameters are as given in the text. The fixed points V_1 , V_2 , V_3 shown refer to the yellow ($V_C = -200$ mV) curve. As V_C is decreased below -200 mV the global maximum becomes the secondary maximum and vice-versa. Increasing V_c above -100 mV, the secondary maximum eventually disappears, at which point there is no kink solution.

The kink solution displayed in Fig. 1 corresponds, in terms of (5), to the particle (of coordinate φ) starting with zero velocity at the maximum $\varphi = V_1$ and arriving (after an infinite time) at the secondary maximum $\varphi = V_3$, also with zero velocity. The value of the dissipation parameter u for which this is possible corresponds to the propagation velocity of the kink. Different velocities are possible transiently, for example, a kink initially steeper than the asymptotic shape will initially travel faster, and slow down as it attains the stable shape and velocity. This "shaping" of the signal expresses the existence of a

stable, unique solitary wave solution. It motivated the electronic realization of an axon, and the corresponding influential dynamical system model, by Nagumo et al [11]. Varying the clamp voltage V_c modifies the potential F , and the kink velocity u changes correspondingly, as shown in Fig. 2. For increasing V_c , the difference $F(V_1) - F(V_3)$ increases, while the secondary maximum at $V = V_3$ becomes less pronounced (Fig. 3). Correspondingly, the kink velocity increases. At a critical clamp value $V_c \approx -92.8$ mV the secondary maximum disappears (the minimum at V_2 becomes an inflection point, then reverses curvature), so no kink solution exists for higher clamp voltages. Conversely, as V_c is decreased, the difference $F(V_1) - F(V_3)$ decreases, goes through zero and becomes negative. Correspondingly the kink velocity also goes through zero and then reverses sign. In short, $F(V_1) - F(V_3)$ increases monotonically with increasing V_c , as does the kink velocity u . There is a maximum positive velocity and a maximum negative velocity (the two are not the same). There is a particular clamp voltage ($V_c \approx 244.0$ mV with our parameters) such that the kink is stationary ($u = 0$). Trivially, for each right-moving kink there is an identical mirror-image left-moving kink, if one inverts the boundary conditions at infinity. From Fig. 3 we also see that two more kink solutions exist, one connecting the maximum at V_1 with the minimum at V_2 (evidently travelling at a faster speed compared to the kink connecting V_1 and V_3), and a third one connecting V_3 and V_2 . These solutions are linearly unstable, because the fixed point at V_2 is unstable; thus they would not be observed experimentally. However, they can still be "observed" numerically, as we see below.

It is interesting to put this problem in a "normal form", and see the connection to other kinks in condensed matter physics. The simplest function F in (5) which supports a kink solution of (3) has a maximum and a minimum, i.e. a cubic non-linearity. A kink solution exists connecting the maximum and the minimum, but it is unstable as the minimum is an unstable fixed point. The next simplest case is that F has three extrema; assuming a single control parameter, we may write:

$$F(V) = a \left[2(1 - \alpha)V^2 + \frac{4}{3}\alpha V^3 - V^4 \right] \quad (6)$$

$a > 0$, $\alpha \leq 1$ where we put one stable fixed point at $V_1 = 1$ and the unstable fixed point (the minimum of F) at $V_2 = 0$. The third (stable) fixed point is at $V_3 = (\alpha - 1)$. This is not the most general form: the choice $V_2 = 0$ forces F to be an even function at the "coexistence point" $\alpha = 0$, as we discuss below; however, this choice allows to discuss unstable kink solutions also. Apart from this difference, this situation corresponds to (4); the parameter α has the role of V_c/V_N , if χ_c/χ is fixed. For $-1 < \alpha \leq 1$ a stable kink with $V(x \rightarrow -\infty) = V_1$ and $V(x \rightarrow +\infty) = V_3$ exists, travelling with a speed u which increases monotonically with increasing α . The stationary kink is obtained for $\alpha = 0$;

for $\alpha > 0$ the kink travels to the right and for $\alpha < 0$ to the left. The simplest stable kink is thus a solution of:

$$\frac{\partial V(x, t)}{\partial t} - \frac{\partial^2 V}{\partial x^2} = 4a[(1 - \alpha)V + \alpha V^2 - V^3] \quad (7)$$

The cubic nonlinearity is a feature of several reduced parameters models of nerve excitability, notably Fitzhugh's "BVP model" [10], and indeed of the original Van der Pol relaxation oscillator [13], in appropriate coordinates. Two further kink solutions of (7) exist, connecting V_1 and V_2 , and V_3 and V_2 . These are linearly unstable, but they can still be obtained numerically, with the trick of arranging for the unstable fixed point to be at $V = 0$, as we did in (6). In this way, one can even discuss collisions between different kinks: the only non-trivial example stemming from (6) is shown in Fig. 4.

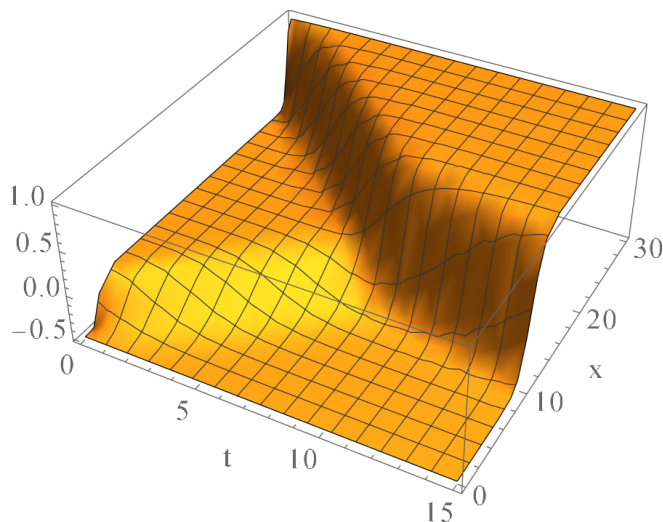


FIG. 4. A 3D plot showing the collision of two different kinks. They are obtained integrating (7) with $a = 0.5$, $\alpha = 0.5$, and appropriate initial conditions. Notice the velocity change after the collision. However, these kinks are linearly unstable and so would not be observed experimentally.

Namely, the kink connecting V_1 and V_2 collides with the kink connecting V_3 and V_2 travelling in the opposite direction, resulting in the stable kink connecting V_1 and V_3 in the final state.

To recapitulate: the fixed points of (3) are uniform, time-independent solutions which we might call "phases". Two fixed points can be connected by a kink. The fixed points are zeros of g , i.e. extrema of F , but the stable fixed points are maxima of F while the unstable ones are minima. For the purpose of classifying, F is analogous to minus the free energy of a Landau theory describing a corresponding phase transition. The stationary kink ($\alpha = 0$ in (6)) is the interface separating two coexisting phases. For $\alpha \neq 0$, one of the two phases is more stable and grows at the expense of the other (i.e. the kink moves). However, we must remember that our system

is never in thermodynamic equilibrium. Even when the kink is stationary, there are macroscopic currents in the system (the clamp current and the channels current), and detailed balance is violated. The function F derived from (4), which is shown in Fig. 3, has the same general form as (minus) the mean field free energy which describes the nematic - isotropic transition in liquid crystals [5], or also the liquid - gas transition. For the former, and following the notation in [5], the free energy f as a function of the order parameter S is:

$$f = \frac{1}{2}a(T - T^*)S^2 - wS^3 + uS^4 \quad (8)$$

where $S = P_2(\cos\theta)$, P_2 the Legendre Polynomial of order 2 and θ the angle between the molecular axis and the director vector. For fixed V_c , the evolution of $-F$ for varying χ_c/χ (where F is the primitive of (4)) mirrors the evolution of (8) for varying temperature T . Namely, for small values of χ_c/χ there is a global minimum at positive V (i.e. channels essentially open) and a secondary minimum at negative V (channels essentially closed). Increasing χ_c/χ one reaches a coexistence point where $-F$ has the same value at the two minima, after which the global minimum is at negative V and the secondary minimum at positive V (Fig. 3), i.e. the stable phase is with channels essentially closed. As in (8) there are limits of meta-stability where the secondary minimum disappears. If we allow V_c as a second control parameter, we find a coexistence line in the $V_c - \chi_c/\chi$ plane ending in a critical point, i.e. the phenomenology of a liquid - gas transition. For parameter values on the coexistence line, the kink is stationary.

For the case of the stationary kink, one can write an implicit formula for the shape: with $u = 0$, multiplying (5) by φ' and integrating from $-\infty$ to x , with the boundary conditions $\varphi' \rightarrow 0$, $\varphi \rightarrow \varphi_1$ for $x \rightarrow -\infty$ one finds

$$\frac{d\varphi}{\sqrt{-F(\varphi) + F(\varphi_1)}} = -\sqrt{2} dx \quad (9)$$

For the stationary kink of (7), which occurs for $\alpha = 0$, we have $F(\varphi) = a(2\varphi^2 - \varphi^4)$, the maxima of F are at $\varphi = \pm 1$, and integrating (9) we find $\varphi(x) = \tanh(-\sqrt{2a}x)$. This is the same kink as in the mean field theory of the Ising ferromagnet, separating two domains of opposite magnetization [5]. It has a special symmetry (inversion about its center), stemming from the symmetry of this particular F , which is an even function at the coexistence point $\alpha = 0$. The function F derived for the Artificial Axon from (4) has no such symmetry, and correspondingly the stationary kink is not inversion symmetric about its center, as Fig. 1 shows. For this kink too an analytic expression can be obtained from (9) in terms of special functions.

Conclusions. We have discussed the occurrence of travelling kink solutions in a dynamical system which repre-

sents a space extended Artificial Axon. We considered the simplest limit: "fast" channels described by an equilibrium opening probability $P_O(V)$. Even so, the velocity of the kink represents a non trivial eigenvalue problem (5). More generally, introducing channel dynamics increases the dimensionality of the dynamical system and leads to more structure (oscillations, limit cycles i.e. action potentials) as is well known. We point out a connection to similar kinks in other areas of condensed matter physics: some questions which can be asked of these systems are similar, for instance, effects beyond mean field [6, 14]. For us, this means replacing the uniform channel conductance with a space distribution of point - like

channels, eventually interacting, eventually mobile. Introducing channel dynamics (see e.g. [15, 16]), it may be interesting to extend this study to pattern formation in 2 space dimensions. In general, this system may inspire the construction of new reaction - diffusion systems [17] with interesting spatio - temporal dynamics.

ACKNOWLEDGMENTS

This work was supported by NSF grant DMR - 1809381.

-
- [1] A. Ariyaratne and G. Zocchi, J. Phys. Chem. B **120**, 6255 (2016).
 - [2] H. G. Vasquez and G. Zocchi, EPL **119**, 48003 (2017).
 - [3] G. Marmont, J Cell Comp. Physiol. **34**, 351 (1949).
 - [4] C. Koch, *Biophysics of Computation* (Oxford University Press, 1999).
 - [5] P. Chaikin and T. Lubenski, *Principles of condensed matter physics* (Cambridge University Press, 1995).
 - [6] F. Buijnsters, A. Fasolino, and M. Katsnelson, Phys. Rev. Lett. **113**, 217202 (2014).
 - [7] H. Kolar, J. Spence, and H. Alexander, Phys. Rev. Lett. **77**, 4031 (1996).
 - [8] H. Rotermund, S. Jakubith, A. von Oertzen, and G. Ertl, Phys. Rev. Lett. **66**, 3083 (1991).
 - [9] A. L. Hodgkin and A. F. Huxley, J. Physiol. (Lond.) **117**, 500 (1952).
 - [10] R. Fitzhugh, Biophys. J. **1**, 445 (1961).
 - [11] J. Nagumo, S. Arimoto, and S. Yoshizawa, Proceedings of the IRE **50**, 2061 (1962).
 - [12] H. G. Vasquez and G. Zocchi, Bioinspiration and Biomimetics **14**, 016017 (2019).
 - [13] B. Van der Pol, Phil. Mag. **2**, 978 (1926).
 - [14] F. Buijnsters, A. Fasolino, and M. Katsnelson, Nature **426**, 812 (2003).
 - [15] C. Morris and H. Lecar, Biophys. J. **35**, 193 (1981).
 - [16] Z. Pi and G. Zocchi, arXiv:2012.00221 (2020).
 - [17] V. K. Vanag and I. R. Epstein, Phys. Rev. Lett. **92**, 128301 (2004).